

CHAPTER II

LITERATURE REVIEWS

2.1 Carbon allotropes

Carbon is the base element for all life on earth. In the past fifty years, many carbon allotropes, including single and multiwalled carbon nanotubes (SWCNTs and MWCNTs, respectively)¹, spherical buckyballs or fullerenes², giant fullerenes^{3,4}, graphene sheets⁵, graphene nanoribbons⁷, carbon onions and cones³, and bud-like aggregates¹¹, have drawn many research interests¹². The most common form of carbon is graphite. The three-dimensional graphite consists of stacked sheets of carbon with a hexagonal structure. Under high pressure condition, a metastable form of carbon, diamond, is formed. The carbon atoms are arranged in a variation of the face-centered cubic crystal structure called a diamond lattice. A single graphitic layer is composed of carbon atoms arranged in a honeycomb-like lattice with a carbon-carbon bond length of 0.142 nm^{13 15}. Two dimension carbon networks of graphene is actually the building block of various architectures such as carbon nanotube and fullerene (Figure 2.1)¹³. It has been claimed that purely 2-D crystalline planes of atoms were thermodynamically unstable^{6 13 15} and will form into 3-D architecture. For instance, carbon nanotubes can be formed from graphene sheets which are rolled up to form tubes.



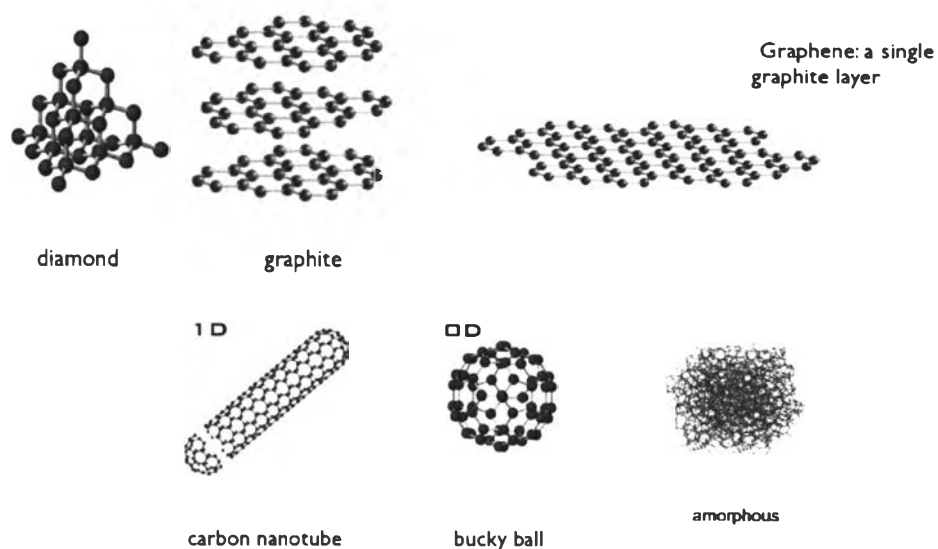


Figure 2. 1 Structure of carbon allotropes

2.2 Usage of carbon allotropes

Owing to their unique electrical, thermal, and mechanical properties, carbon-based nanomaterials have attracted a lot of attention in recent years. Two dimensional materials, graphene oxide and carbon nanotube, exhibit remarkable structural, electronic^{14 16}, mechanical^{16 17}, and optical^{18 19} properties. The graphene oxide and carbon nanotube were developed as materials for many industries, such as microelectronic^{18 20}, biosensor²¹, polymer composites²² and solar cells¹⁸. Moreover, graphene oxide and carbon nanotube, have been to interest in biological field such as biosensor, cellular trafficking and drug delivery system. Because of the surface structure of carbon-based materials which is π -conjugated structure has ability to absorbed hydrophobic bioactive^{35 36}. The reactive oxygen containing functional groups (e.g., hydroxyl, epoxide and carbonyl groups) on their surface also can be modified for enhanced its ability including biocompatibility, solubility and fluorescence property.

In sensor field, Schedin and co-worker³⁷ used the graphene in sensing application for NO_2 , NH_3 , H_2O and CO detection. Hu and co-worker³⁸ prepared graphene nanosheets-gold (GNS-Au) nanocomposite by microwave radiation for



modified glassy carbon electrode. This material showed enhanced electrochemical response and highly sensitive electrochemical sensor. Liu and co-worker prepared modified graphene oxide (GO) as enzyme electrode for biosensor²¹. Chang and co-worker³⁹ also developed the dye labeled aptamer assembled graphene for a highly sensitive and specific fluorescence resonance energy transfer (FRET) aptasensor for thrombin detection.

In the electronic field, carbon-based material has been used in place of indium tin oxide (ITO). Indium tin oxide (ITO) has been widely used as an electrode material in optoelectronic devices because of its high conductivity, good transmittance, and suitable work function. On the other hands, indium has limited availability on the earth. Thus, carbon-based material becomes alternative supply for the fabrication of devices such as organic light-emitting diodes and solar cells^{18 38 40}. In 2008 Wang and co-worker¹⁸ prepared ultrathin graphene films that possess transparent, high chemical and thermal stabilities, and excellent conductive properties. They demonstrated that graphene films can be used as an alternative to the ubiquitously employed metal oxides window electrodes for solid-state dye-sensitized solar cells. Tung and co-worker⁴⁰ prepared a nanocomposite of graphene and carbon nanotubes hybrid for use as for high-performance transparent conductors in solar cell.

In biological field, In 2007 Lacerda and co-worker³² synthesized ammonium functionalized carbon nanotubes (SWNT-NH³⁺) for cell imaging. In 2009, Heister and co-worker³³ showed the triple functionalized carbon nanotubes which is cancer specific antibody, anticancer drug and fluorescence dye. In 2012, Ma and co-worker⁴¹ synthesized the multifunctional superparamagnetic graphene oxide-iron oxide hybrid nanocomposite (GO-IONP) functionalized with PEG and loaded with doxorubicin (DOX) for targeted drug delivery and bioimaging applications.

2.3 Synthesis of various carbon allotropes

Generally, the carbon nanoparticles, carbon nanotubes and fullerene, are synthesized by Arc discharge⁴², chemical vapor deposition (CVD)²³, and laser ablation^{43 44}. In 1992 Ebbesen and Ajayan demonstrated growth and purification of



high-quality MWNTs at the gram scale via arc discharge method. For the growth of single-wall tubes, a metal catalyst is needed in the arc discharge system. Bethune and co-workers⁴⁵ were successfully synthesized large amounts of SWNTs by arc discharge. Thess and co-workers⁴³ used laser ablation (laser oven) method to upscale the synthesis of SWNTs to 1–10 g. With the same method, laser-ablation, Iijima and co-worker⁴⁶ found a new carbon allotrope, graphitic carbon nanohorns. The product has size around 80 nm. The TEM image showed an aggregate of many horn-shaped sheaths of single-walled graphene sheets.

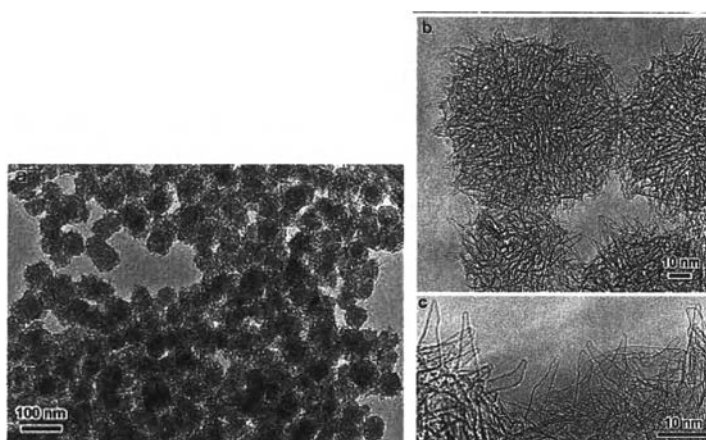


Figure 2. 2 TEM micrograph of graphitic carbon nanohorns; (a) A TEM micrograph shows a graphitic carbon product. (b) A magnified TEM micrograph of the graphitic carbon particles shows aggregations of tubule-like structures sticking out of the particle surface. (c) A highly magnified TEM micrograph of the edge regions of the graphitic particles shows conical horn-like protrusions of up to 20 nm long on the particle surface⁴⁶

In relatively large (gram) amounts, Arc discharge and laser ablation were proposed as the first methods that allowed synthesis of SWNTs⁴⁴. Both methods involve the condensation of hot gaseous carbon atoms generated from the evaporation of solid carbon. The arc and laser methods can produce only carbon nanotubes tangled into bundles. The arc and laser methods have not been controllable synthesis on substrates with ordered nanotube structures. Then the chemical vapor deposition (CVD) method which is the decomposition of a gaseous or

volatile compound of carbon and catalyzed by metallic nanoparticles, is used for the synthesis carbon nanotube. This method has become the most important commercial method for SWCNT production^{23 44 47 48}. In 1998, Kong and co-worker⁴⁷ synthesized high-quality single-walled carbon nanotubes SWNT by CVD method of methane on supported FeO catalysts. In 2002 Huang and co-worker²³ synthesized carbon nanotubes by CVD method with using various catalysts such as nickel, iron and cobalt. In 2006 Deck and co-worker⁴⁹ synthesized carbon nanotubes (CNTs) using a vapor-phase CVD method with a wide variety of transition metals as potential growth catalysts. The synthesis of carbon allotrope usually leaves some trace amounts of catalysts such as nickel, iron and cobalt in the materials. This hindered medical applications of the obtained materials.

At present, graphene and graphene oxide can be synthesized by simple oxidizing the inexpensive graphite^{24 50 51 52 53 54}. The obtained graphene and graphene oxide can be easily purified from oxidizing agents. In 1860, Brodie⁵⁰ synthesized graphene oxide by oxidizing graphite with potassium chloride and fuming nitric acid for 4 days. The most important and widely applied method for the synthesis of graphene oxide (GO) was developed by Hummers and Offeman²⁴. At present most chemical syntheses of carbon-based materials are typically achieved by Hummers method^{24 51} or modified Hummers methods^{52 53 54}. The methods involved strong oxidizing reaction by potassium permanganate in acidic environment. According to Hummer and co-worker in 1958²⁴, they synthesized graphitic oxide from graphite through an oxidation reaction using sulfuric acid, sodium nitrate and potassium permanganate. The result showed graphitic oxide with 2.25 of C to O ratio. This method has important advantages over previous techniques. Firstly, the reaction can be completed within a few hours. Secondly, KMnO_4 was used instead of KClO_3 to improve the reaction safety, avoiding the evolution of explosive ClO_2 . Thirdly, NaNO_3 was used instead of fuming HNO_3 to eliminate the formation of acid fog.

In 1998, Lef and co-worker⁵⁵ synthesized graphite oxide by oxidation reaction follow by Hummer method. The results showed successful oxidized graphite which is carboxyl and hydroxyl functional groups. Stankovich and co-worker⁵³ synthesized graphene oxide by Hummers method and then reduced graphene oxide with



hydrazine hydrate. The resulting graphene was sheet-like with 2 nm thick and they showed aggregation.

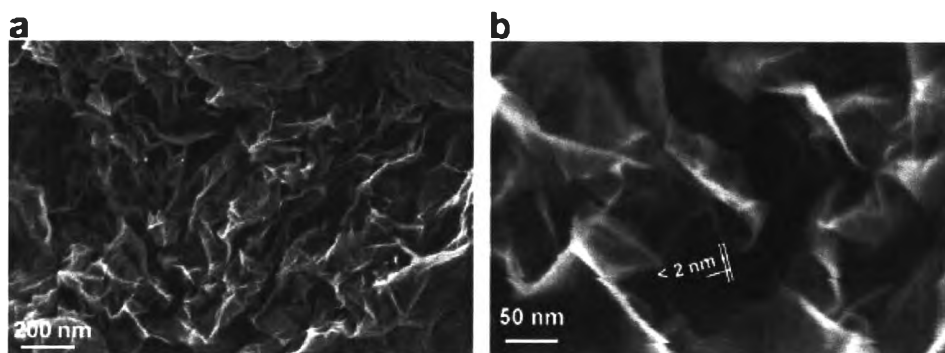


Figure 2.3 SEM images of aggregated reduced GO sheets (a) and thickness of 2 nm (b)⁵³.

Even though, the Hummers method gave many advantages such as fast, easy purify, and safety, the oxidation process can still be modified depending on the aim of production, such as required functional group, shapes and particle size of the product. Wang and co-worker⁵⁶ proposed facile synthesized graphene oxide nanosheets via modified Hummers method using oxidation, ultrasonic exfoliation, and chemical reduction. TEM image showed graphene oxide nanosheets with size in range 10 to 100 nm. Cataldo and co-worker⁵⁷ synthesized graphene nanoribbons using oxidative tearing of single-wall carbon nanotubes (SWCNTs). SWCNTs was oxidized with modified Hummer's method, nitric acid and sulfuric acid (1:3 volume ratio), followed by ultrasonication. Macano and co-worker⁵⁸ found that excluding the NaNO_3 , increasing the amount of KMnO_4 , and performing the reaction in a 9:1 mixture of $\text{H}_2\text{SO}_4/\text{H}_3\text{PO}_4$ improves the efficiency of the oxidation process for graphene oxide production. Chen and co-worker⁵⁹ proposed an improved Hummers method without using NaNO_3 to synthesize graphene oxide. This method eliminated the evolution of $\text{NO}_2/\text{N}_2\text{O}_4$ toxic gasses problem whereas the yield of product is still same. Wang and co-worker⁷ synthesized carbon nanotubes (CNT) from graphene oxide (GO) nanosheets by ultrasonating GO in 70% nitric acid. They found that this method can generate many form of carbon-based materials, CNT, carbon nanoparticle-like onion, and nanoribbons. They separated and purified each form by centrifugation.

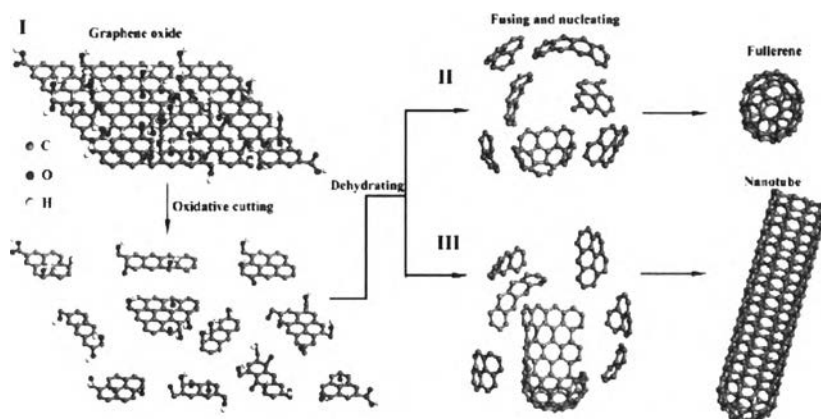


Figure 2. 4 Schematic illustration of the mechanism for transforming GO nanosheets into carbon nanoparticles and nanotubes following their ultrasonication in acid; (I) Oxidative cutting of graphene oxide produces PAH molecules in concentrated HNO_3 . In the dehydrating acidic medium, the polyaromatic fragments fuse and nucleate into (II) carbon nanoparticles or (III) nanotubes via acid-catalyzed intramolecular or intermolecular dehydration reactions⁷

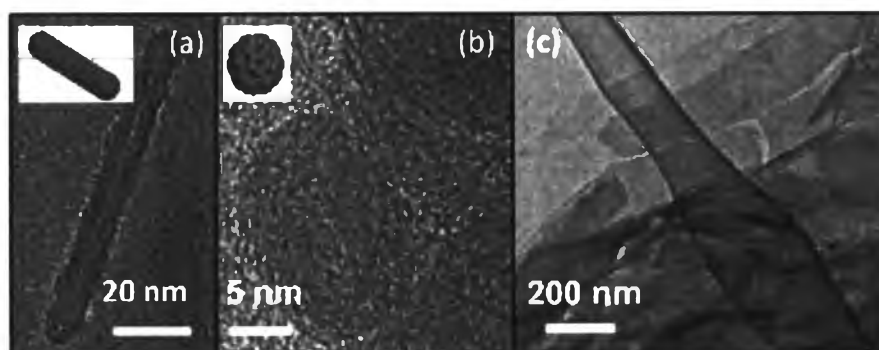


Figure 2. 5 TEM images showing (a) a CNT, (b) carbon nanoparticles, and (c) nanoribbons obtained by sonicating GO sheets in 70% HNO_3 at RT⁷

Higginbotham and co-worker²⁵ improved Hummers method by modifying various factors, including solvent, reaction time, reaction temperature and oxidizing agent. The products from the reactions were consisted of different degree of oxidized nanoparticulates, for instance, single-wall carbon nanotubes (SWCNT), multi wall-carbon nanotubes (MWCNT), monolayer nanoribbons and multiple layer graphene oxide sheets. The products were partially purified by filtration.

2.4 Modification of carbon allotropes

Many carbon allotropes usually tend to aggregate in both physiological solutions and hydrophobic environment due to non-specific binding^{35 36}. This is one of many drawbacks of carbon allotropes in drug delivery application. To solve these problems, the functionalization of carbon allotropes nanoparticles has been pursued [64-83]. Surface of carbon allotropes contains reactive oxygen-containing functional groups (e.g., hydroxyl, epoxide and carbonyl groups). Therefore, a wide range of reactions can be activated from these groups. These groups enable carbon allotropes nanoparticles to be functionalized through covalent and non-covalent approaches. For instance, PEGylated-grafted graphene^{60 61 62} [64-66] and graphene oxide^{41 63}, poly(vinyl alcohol) (PVA)-grafted graphene oxide⁶⁴, polyethylenimine (PEI)-grafted graphene oxide^{65 66}, poly(N-isopropylacrylamide) (PNIPAM)-grafted graphene⁶⁷, polysebacic anhydride (PSA)-grafted graphene oxide⁶⁸, poly(sodium 4-styrenesulfonate) (PSS)-grafted SWCNT⁶⁹, poly(vinyl pyrrolidone) (PVP)-grafted SWCNT⁷⁰, chitosan (CS)-grafted graphene⁷¹ and graphene oxide^{72 73}, amphiphilic copolymers-grafted graphene oxide^{74 75}, sulfonic acid groups-grafted graphene oxide⁷⁶ and amino groups-grafted graphene oxide⁷⁷, peptide conjugated CNT⁷⁸ have been synthesized to increase their biocompatibility.

In 2008 Liu and co-worker⁶⁰ prepared graphene oxide by oxidizing graphite using a modified Hummer's method and then functionalized graphene oxide with PEGylation for improve water solubility. PEGylated nanographene oxide (NGO-PEG) readily complexes with a water insoluble aromatic molecule SN38, a camptothecin (CPT) analogue, via noncovalent van der Waals interaction. In 2009 Shen and co-worker³⁰ modified acid-treated multi-walled carbon nanotubes (MWCNTs) with polyethyleneimine (PEI) by covalently bonded for use in environmental and biomedical applications. The result showed that the functionalized MWCNTs are water-soluble and stable.



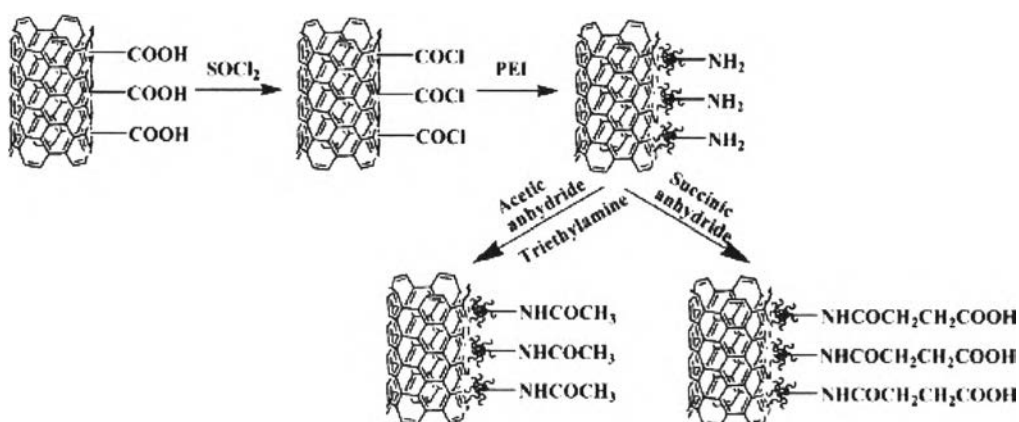


Figure 2. 6 Schematic representation of reactions to modify MWCNTs through PEI-mediated functionalization³⁰

He and co-worker⁷⁹ modified many kind of graphene nanosheets based on nitrene chemistry, allowing various functional moieties (e.g., hydroxyl, carboxyl, amino, bromine, long alkyl chain, etc.) and polymers (e.g., poly(ethylene glycol), polystyrene) to covalently and stably anchor on graphene. The functionalized graphene nanosheets exhibited easily dispersible than those of graphene oxide.

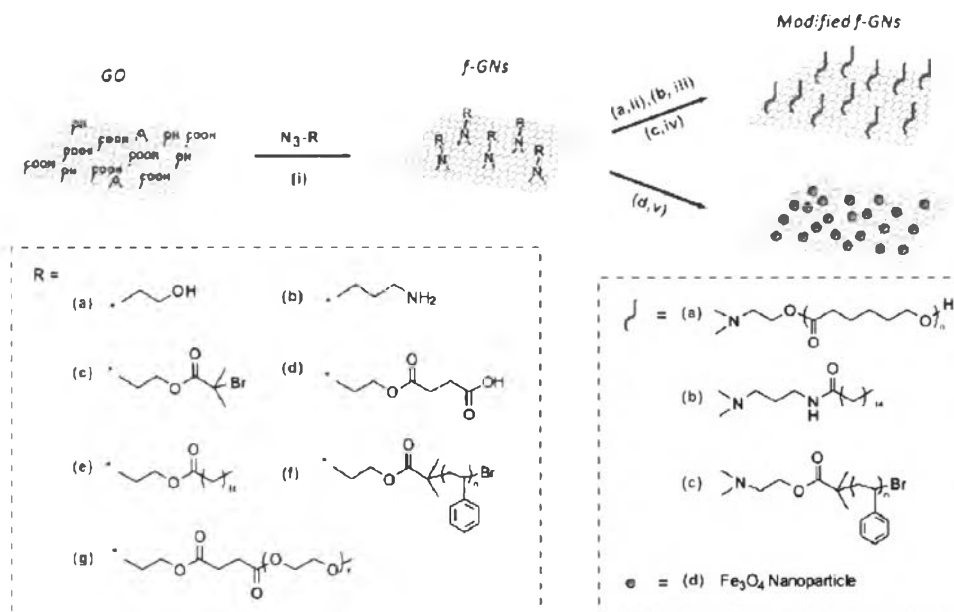


Figure 2. 7 General strategy for the preparation of functionalized graphene nanosheets (f-GNs) by nitrene chemistry and the further chemical modifications⁷⁹

In 2011, Pan and co-worker⁶⁷ modified covalently functionalized graphene sheets by grafting a well defined thermo-responsive poly(N -isopropylacrylamide) (PNIPAM) via click chemistry. The PNIPAM-grafted graphene sheets (PNIPAM-GS) showed good solubility and stability in physiological solutions and exhibited phase transition at 33 °C.

Not only covalent interaction but non-covalent interaction also becomes alternative methods to protect the structures and properties of carbon-based nanoparticles. The solubility of carbon-based nanoparticles can be improved without any chemical reaction. The commonly used non-covalent interaction is surfactant dispersion^{80 81}, π - π stacking with aromatic compounds⁸², and polymer wrapping^{80 81 82 83}. By increasing solubility and stability in physiological solutions, the functionalized carbon allotropes nanoparticles could indirectly enhance the dissolution of the water-insoluble bioactive drugs. In 2003 Islam and co-worker⁸⁰ reported process to water solubilize high weight fraction single-wall carbon nanotubes by the nonspecific physical adsorption of sodium dodecylbenzene sulfonate. Moore and co-worker⁸¹ also improved the solubility of single-walled carbon nanotubes (SWNTs) in aqueous media using various anionic, cationic, nonionic surfactants and polymers. A nonionic surfactant and polymer showed the ability to suspend particles due to increasing of the hydrophilicity with higher molecular weights.

2.5 The use of carbon allotropes as carriers

Recently, various carbon allotropes were intensively studied in biomedical applications such as ability to deliver bioactive compounds^{35 36}. According to the surface structure of carbon allotropes the planar structure and π -conjugated structure possesses ability to immobilize bioactive compound with Van der Waals interactions. The carbon allotropes have ability to immobilize a large number of substances, including metals, drugs, biomolecules and fluorescent molecules. In case of bioactive loading, it can be easily absorbed hydrophobic bioactive and molecules, doxorubicin^{35 84}, paclitaxel³⁶ and camptothecin (CPT)⁶⁴ via π - π stacking and hydrophobic interactions. In 2008, Sun and co-worker⁸⁵ synthesized and explored the biological applications of nano-graphene oxide (NGO). The NGO was loaded with



doxorubicin via simple physical absorption through π - π stacking. Yang and co-worker³⁵ synthesized doxorubicin-loaded graphene oxide. The result showed 2.35 mg/mg of doxorubicin-loaded graphene oxide. The doxorubicin releasing was depended on pH.

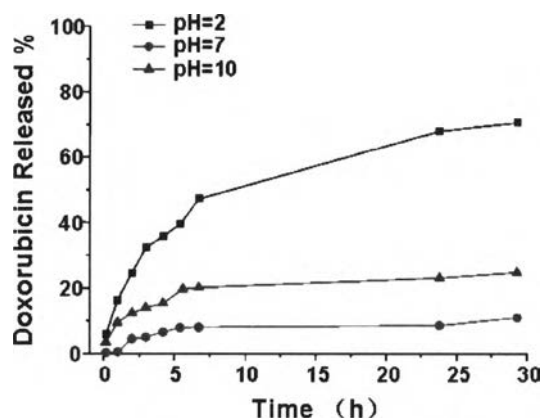


Figure 2. 8 The release of doxorubicin on graphene oxide at different pH values³⁵

Liu and co-worker³⁶ synthesized paclitaxel-labeled carbon nanotubes and comparing their anticancer activity to that of free paclitaxel. The result showed that paclitaxel-labeled carbon nanotubes could inhibit the growth of cancer cell better than free paclitaxel. The paclitaxel-labeled carbon nanotubes showed pro-longed life in blood circulation. Sahoo and co-worker⁶⁴ functionalized carbon nanomaterials such as multi-walled carbon nanotubes (MWCNTs) and graphene oxide (GO) with poly(vinyl alcohol) (PVA). Then camptothecin (CPT) was loaded into carbon-based nanomaterials through π - π interactions. The anticancer test investigated that CPT-loaded carbon-based nanomaterials show capability to kill human breast and skin cancer cells. Depan and co-worker⁷¹ prepared doxorubicin loaded graphene oxide (GO) for drug delivery system by strong π - π stacking interaction. The doxorubicin loaded graphene oxide (GO) enhanced the water stability which is the hydrophilicity. The drug release showed pH-sensitive behavior with higher drug release at pH 5.3.

Furthermore, a number of researchers proposed that the carbon-based nanomaterials also can be protecting bioactive from enzymatic cleavage and

interference with binding proteins. The carbon-based nanomaterials can be absorbing protein, DNA and RNAs by adsorption. Wu and co-worker⁸⁶ developed single-walled carbon nanotubes (CNT) as a carrier for single-stranded DNA probe delivery. They found that CNT protected DNA probes from enzymatic cleavage and interference from nucleic acid binding proteins. Lu and co-worker⁸⁷ reported that the functionalized nanoscale graphene oxide (NGO) possesses efficiently deliver oligonucleotides, molecular beacon, into cells. The result showed that it can protect oligonucleotides from enzymatic cleavage. The MB/NGO complex exhibited improved the transfection efficiency and release of MB during the cell transporting.

The study of the effective carrier system does not only involve the transportation, but also the positive confirmation of the specific location of the drug and the carriers. The advantage of functionalized carbon-based materials could be labeled with fluorescent dyes. In 2007 Lacerda and co-worker³² synthesized ammonium functionalized carbon nanotubes (SWNT-NH³⁺s) with auto-fluorescence property. Tracking the luminescence signal of SWNT-NH³⁺s with CLSM demonstrated that the carbon nanotubes could be taken up into lung cancer cell.

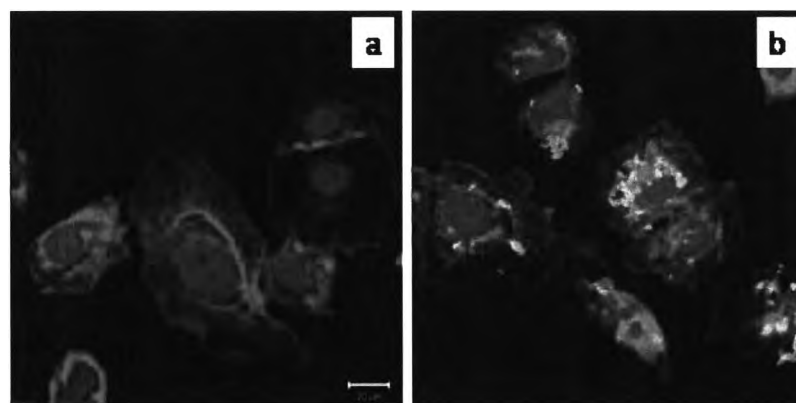


Figure 2. 9 Multiple stain confocal images of lung cancer cells after 2 h incubation (37 °C, 5% CO₂); (a) in the absence of SWNT-NH³⁺s (control) and (b) in the presence of 20 µg of SWNT-NH³⁺s (green) (Scale bar: 20 µm). Cellular membranes are stained in red with WGA-TRITC and nuclei are counterstained in blue with TO-PRO 3³²

In 2009, Heister and co-worker³³ functionalized carbon nanotubes with cancer specific antibody, anticancer drug and fluorescence dye. The CLSM imaging indicated that the particles were translocated into cytoplasm and the drug was released into nucleus.

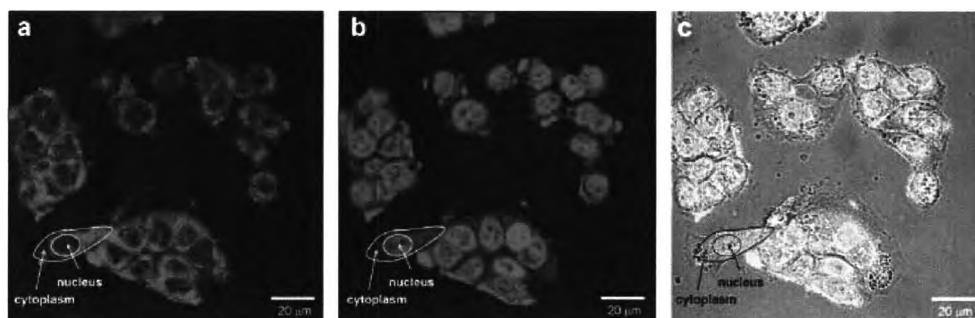


Figure 2. 10 Confocal image of human colon cancer cell line incubated with doxorubicin triple functionalized carbon nanotubes; a) fluorescein-labeled SWCNT (green), b) doxorubicin (red) and c) merged image (co-localized region was showed in yellow)³³

In 2010 Wang and co-worker⁸⁸ modified graphene oxide for applications in bionanotechnology as intracellular monitoring and molecular probing, including DNA sensing, protein assays, and drug delivery. To investigate its ability for molecular probing in living cells, they synthesized an aptamer-carboxyfluorescein (FAM)/graphene oxide nanosheet (GO-nS) nanocomplex. The result showed successfully uptake of aptamer-FAM/GO-nS nanocomplex and cellular target monitoring.

Additionally, in case of usage of modified carbon-based nanomaterials can be control to targeted local. In 2009 Yang and co-worker⁸⁴ prepared superparamagnetic graphene oxide -Fe₃O₄ nanoparticles hybrid (GO-Fe₃O₄) by a simple and effective chemical precipitation method for controlled targeted drug carriers. The GO-Fe₃O₄ hybrid was loaded doxorubicin hydrochloride (DXR) as a model. The GO-Fe₃O₄ hybrid shows before and after loading with the molecule DXR can be moved regularly after congregating. Moreover, GO-Fe₃O₄ hybrid possesses superparamagnetic property and

can congregate under acidic conditions and be re-dispersed reversibly under basic conditions.

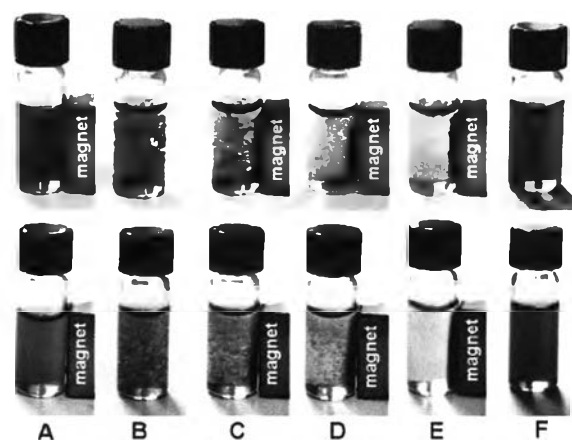


Figure 2. 11 Photographic images of the behaviors of GO-Fe₃O₄ hybrid (upper) and GO-Fe₃O₄ hybrid loaded with DXR (lower) in the magnetic field under different conditions: neutral conditions (A), acidic conditions (pH 2–3) (B–E) and basic conditions (pH 8–9) (F)⁸⁴

In 2012, Ma and co-worker⁴¹ synthesized a multifunctional superparamagnetic graphene oxide–iron oxide hybrid nanocomposite (GO–IONP) which is then functionalized by polyethylene glycol (PEG) polymer. The doxorubicin-loaded GO–IONP–PEG was used as model carriers which enables magnetically targeted drug delivery. The half-maximum inhibitory concentration (IC₅₀) value of GO–IONP–PEG–DOX was 0.52 μmol/L whereas IC₅₀ of free DOX was 0.43 μmol/L. As a result, many modified carbon-based nanomaterials have been developed and synthesized for widespread investigations on their potential bioapplications. In further studies, more efforts should be devoted to demonstrate that carbon nanotubes not only “can be used” but also “are uniquely suited” for various applications in biology and medicine.

2.6 Cytotoxicity of various carbon allotropes

The past few years, the production and novel uses of large quantities of carbon-based nanoparticles are becoming an increasing reality. The potential health risks for these materials have been significantly apprehension. Toxicological studies

have been concerned with virtually uncharacterized. One simple cytotoxicity test involves visual inspection of the cells with bright-field microscopy for changes in cellular or nuclear morphology. Fiorito and co-worker⁸⁹ used this technique when evaluating the cytotoxicity of single-walled carbon nanotubes (SWNTs). However, the majority of cytotoxicity assays usually used colorimetric methods for measure cell death or cell viability. The colorimetric methods can be used for measurement plasma membrane integrity and mitochondrial activity. The 3-(4,5-dimethylthiazol-2-yl)-2,5-diphenyltetrazolium bromide mitochondrial activity (MTT) assay has also become the analysis of cytotoxicity which is measured mitochondrial activity. Magrez and co-worker⁹⁰ studied on cellular toxicity of carbon-based nanomaterials at concentration of 0.02-0.2 $\mu\text{g}/\text{mL}$ using MTT assay. They found that the toxicity of carbon nanotubes increases significantly when carbonyl (C=O), carboxyl (COOH), and/or hydroxyl (OH) groups are present on their surface. In 2007 Wick and co-worker²⁹ studied cytotoxicity of carbon nanotubes which were synthesized by conventional arc-discharge evaporation. The synthesis gave various particles, including, carbon nanotubes, carbon nanotube bundles and carbon nanotube pellets. The cytotoxicity test was analyzed by MTT assay with Mesothelioma cell line (MSTO-211H). The result showed that at concentration of 0-30 $\mu\text{g}/\text{mL}$, the carbon nanotube bundles were less cytotoxic than carbon nanotube agglomerate and carbon nanotube pellet. Simon-Deckers and co-worker⁹¹ studied the response of A549 human pneumocytes after exposure to aluminium oxide or titanium oxide nanoparticles, and to multi-walled carbon nanotubes (MWCNTs) at concentration of 0-100 $\mu\text{g}/\text{mL}$ by MTT assay. The result showed that MWCNTs was more cytotoxic than other nanoparticles. Shen and co-worker³⁰ synthesized polymer-functionalized multi-walled carbon nanotubes (MWCNTs). The amine groups of PEI (polyethyleneimine) on the surface of MWCNTs were reacted with acetic anhydride or succinic anhydride to form MWCNTs with neutral or negative surface charges, respectively. The cytotoxicity study with human thyroid cancer cell line (FRO cell) and human epithelial carcinoma cell line (KB cell) showed that the positively charged MWCNTs are toxic to FRO cell at 10 $\mu\text{g}/\text{mL}$. Neutral and negatively charged MWCNTs are nontoxic to both cell lines at a concentration up to 100 $\mu\text{g}/\text{mL}$. In 2010, Ghosh and co-worker³⁴ synthesized



graphene oxide-*para* amino benzoic acid nanosheet by modified Hummers method using $K_2Cr_2O_7$ as oxidizing agent. The antimicrobial activity of tetracycline loaded nanosheet (GO-PABA-tet nanosheet) was determined in terms of minimal inhibitory concentration. Stability of *p*-amino benzoic acid in aqueous solution was improved by the graphene oxide nanosheets. The minimal inhibitory concentration of this GO-PABA-tet nanosheet was found to be 110 $\mu\text{g/mL}$. Hu and co-worker³¹ synthesized graphene and graphene oxide by Hummers method. The result showed that both nanomaterials were effectively inhibiting the growth of *E. coli* bacteria. The cytotoxicity of graphene oxide sheets in lung cancer cell showed toxicity at 80 $\mu\text{g/mL}$ when incubated for 24 h. Ye and co-worker⁹² studied on toxicity exhibited by carboxylic acid functionalized single-walled CNTs (SWCNTs). The particles size of SWCNTs was diameter of 1–2 nm and mean length of 500 nm. The biological effects of carboxylated SWCNTs in human primary monocytes showed cytotoxicity and led to interleukin-8 (IL-8), interleukin-6 (IL-6) expression, and nuclear factor-kappa B (NF- κ B) activation.

However, the cytotoxicity studies are become most likely not only in vitro but also in vivo studies. As toxicity studies move more into in vivo nanoparticle evaluation, future experiments need to incorporate the effect of nanoparticles to determine the extent of clearance and bioaccumulation. Lam and co-worker⁹³ studied pulmonary toxicity of SWCNT compare with carbon black and silica quartz. The mice were treated with 0.1 and 0.5 mg of materials per mouse and euthanized 7 days and 90 days after single treatment. The result showed that SWCNTs possess more toxic to mouse lungs than carbon black and silica quartz. Warheit and co-worker⁹⁴ studied pulmonary toxicity of SWCNTs compared with quartz particles (positive control), carbonyl iron particles (negative control), phosphate-buffered saline (PBS) + 1% Tween 80, and graphite particles. The mice were treated with 5 mg of materials per mouse. The histopathological evaluation was investigated at 24 h, 1 week, 1 month and 3 months. The result showed that high dose of SWCNTs, produced transient inflammatory cell injury in rat lung. Zhang and co-worker⁹⁵ studied on the distribution and biocompatibility of graphene oxide (GO) in mice by radiotracer technique and a series of biological assays. The results showed GO



remaining in lungs and blood circulation for long time. The pathological organs were unchanged when mice were exposed to 1 mg/ kg body weight of GO for 14 days. Nonetheless, when mice were exposed to 10 mg/ kg body weight, the high accumulation and longtime retention, significant pathological changes, including inflammation cell infiltration, pulmonary edema and granuloma formation were found. Therefore, the usage of carbon-based nanomaterials, it must be proven safe. This review documents the advancement in biomedical application of carbon-based nanomaterials as carriers, and also highlights the toxicity and regulatory aspects of these materials.

2.7 Curcumin delivery



Figure 2. 12 Curcuma longa

Curcumin [1,7-bis(4-hydroxy-3-methoxyphenyl)-1, 6,7-heptadiene-3, 5-dione] is the polyphenol active ingredient derived from the rhizome of turmeric (*Curcuma longa*) (Figure 2.12). The rhizomes of turmeric are consisted of three compounds, curcumin, demethoxycurcumin and bisdemethoxycurcumin. As shown in Figure 2.13, commercial curcumin contains curcumin (~77%), demethoxycurcumin (~17%), and bisdemethoxycurcumin (~3%) as its major components. Chemically, curcumin is quite soluble in organic solvents such as dimethyl sulfoxide, ethanol, and acetone etc., but it is poor water-soluble. The molecular formula and molecular weight of

curcumin are $C_{21}H_{20}O_6$ and 368.37 g/mol, respectively. The maximum absorption (λ_{max}) of curcumin in methanol and acetone are 430 nm⁹⁶ and 415 to 420 nm, respectively. Moreover, it possesses strongly autofluorescence. The autofluorescence activity of curcumin helps identification of the substance inside target cell easier by confocal laser scanning fluorescence microscope (CLSM)^{97 98}.

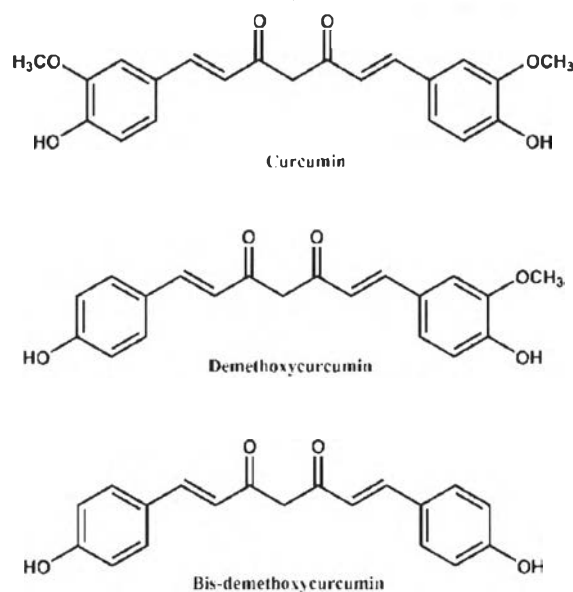


Figure 2. 13 Structure of curcumin, demethoxycurcumin and bis-demethoxycurcumin

Curcumin has many bioactivities such as anticancer^{99 100 101 102} [106-109], anti-inflammatory^{103 104 105}, antioxidant^{103 104 106} antimicrobial¹⁰⁷ and anticarcinogenic^{108 109} etc. Many researches showed reducing blood cholesterol¹¹⁰ and anti-alzheimer activity of curcumin⁹⁸. Various studies have shown that curcumin modulates numerous targets including the growth factors, growth factor receptors, transcription factors, cytokines, enzymes, and genes regulating apoptosis^{111 112}. Curcumin inhibits COX-2 expression¹¹³, inflammatory cytokines, such as IL-1B, and TNF-A^{114 115} and down-regulates activation of c-Jun N-terminal kinase (JNK), activated protein-1 (AP-1) and nuclear factor kappa B (NF- κ B)¹¹⁶. These activities have been demonstrated both in cultured cells and in animal models. However, the reasons for reduced bioavailability of curcumin are water insolubility, poor absorption, high rate of metabolism^{117 118}, inactivity of metabolic products and/or rapid elimination and clearance from the body^{119 120}. Many studies related to absorption, distribution,

metabolism and excretion of curcumin have revealed water insolubility, poor absorption and rapid metabolism of curcumin that severely curtails its bioavailability.

To solve the problem of curcumin, the use of liposomal curcumin, curcumin nanoparticles, the use of curcumin phospholipid complex, and the use of structural analogues of curcumin were demonstrated. To enhance the bioavailability, medicinal value and application of this interesting molecule, many techniques appear to provide longer circulation, better permeability and resistance to metabolic processes¹²¹. In 2007 Bisht and co-worker¹²² synthesized polymeric nanoparticle for encapsulated curcumin with random copolymers of Nisopropylacrylamide (NIPAAm), with N-vinyl-2-pyrrolidone (VP) and poly(ethyleneglycol)monoacrylate (PEG-A). To study therapeutic efficacy in vitro, blockade of nuclear factor kappa B (NF- κ B) activation, and down regulation of steady state levels of multiple proinflammatory cytokines (IL-6, IL-8, and TNF α), nanocurcumin showed similar result with free curcumin. Sahu and co-worker¹²³ encapsulated curcumin into palmitic acid conjugated methoxy poly(ethylene glycol) micelle. The curcumin activity was studied in Epidermoid cervical carcinoma cells at concentration 1-30 μ M. The result showed IC₅₀ of free curcumin and curcumin encapsulated micelle of 14.32 and 15.58 μ M, respectively, at incubation time of 48 h. The micellar nanoencapsulation improved the aqueous solubility and bioavailability of curcumin. Anand and co-worker¹²⁴ prepared a biodegradable nanoparticle (NP) formulation of curcumin using PLGA-PEG and tested its bioavailability and effects on cells growth. The result showed that curcumin (NP) exhibited very rapid and more efficient cellular uptake than free curcumin. Moreover, curcumin (NP) showed more potent inducing apoptosis of leukemic cells and in suppressing proliferation of various tumor cell lines. Das and co-worker¹²⁵ synthesized alginate-chitosan-pluronic composite nanoparticles to encapsulated curcumin, using ionotropic pre-gelation method together with polycationic cross-linking. The curcumin activity was studied in cervical cancer cells (HeLa cell) at concentration 2-14 μ M after incubated 24 h. The result showed IC₅₀ of free curcumin and curcumin encapsulated composite nanoparticles of 13.28 and 14.34 μ M, respectively. In 2011, Sanoj Rejinold and co-worker⁹⁹ encapsulated curcumin using chitosan-g-poly(N-vinylcaprolactam) (TRC), a thermoresponsive



polymer. The curcumin activity was studied in cancer cells at concentration 0-1 mg/mL. At 24 h of incubation, curcumin encapsulated-TRC nanoparticles gave higher anticancer efficiency than free curcumin. In 2012 Bansal and co-worker¹²⁶ prepared curcumin loaded polymeric nanoparticles to solve limitation of anti-inflammatory and anti-proliferative activities of curcumin. The result found that curcumin loaded polymeric nanoparticles exhibited diffusion-mediated biphasic release pattern with around 2-fold higher in vivo release. These curcumin loaded polymeric nanoparticles showed higher curcumin concentrations in plasma, brain and to some extent in liver over a period of 3 months. From these results, the higher and extent concentrations of curcumin are a viable alternative for delivery of curcumin to various organs like brain for patients suffering with Alzheimer's disease and/or brain gliomas.

Not only encapsulation techniques could enhance bioavailability and solubility but modification of curcumin could also improve those properties. Recent year, Parvathy and co-worker¹²⁷ improved water solubility of curcumin by modified functional group with suitable amino acid derivatives. Several amino acid conjugates of curcumin were soluble in water at 1– 10 mg/ml concentrations. The analysis of antioxidant assays showed that curcumin derivatives with alkyl-substituted amino acids, such as alanine, valine, serine and cysteine, exhibited smaller IC₅₀ values than curcumin. The antimutagenicity test also showed that the derivatives showed an effect stronger than or, in a few cases, similar to curcumin. Tang and co-worker⁹⁷ prepared a polymer-drug conjugates with the high molecular weight curcumin polymers (polycurcumins) by condensation polymerization of curcumin. The polyacetal-based polycurcumin (PCurc 8) showed highly cytotoxic to SKOV-3, OVCAR-3 ovarian cancers, and MCF-7 breast cancer cell lines. From intercellular uptake imaging, PCurc 8 was quickly taken up by cancer cells through their lysosomes. In vivo, intravenously (i.v.) injected PCurc 8 shows remarkable antitumor activity in SKOV-3 intraperitoneal (i.p.) xenograft tumor model.



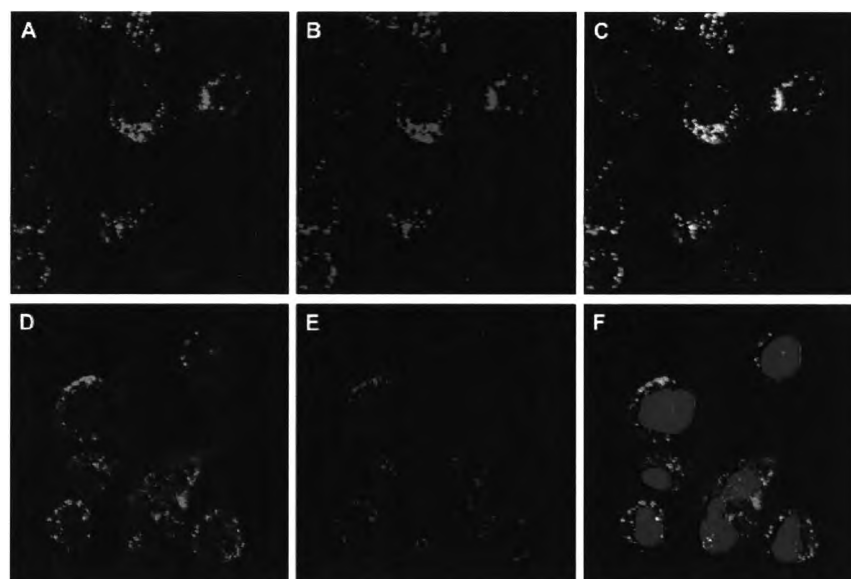


Figure 2. 14 Intracellular distribution of PCurc 8 observed by confocal microscopy. SKOV-3 cells were treated PCurc 8 at 25 mg/mL for 2 h (A-C) and 24 h (D-F). Images were taken from the PCurc 8 channel (Left column, green) and the LysoTracker channel (middle column, red), and overlapped of two channels (the right column). The image F is also overlapped with the nuclear dye channel (Blue)⁹⁷

In 2012, Amomwachirabodee and co-worker¹²⁸ synthesized curcumin (CUR) derivative as carriers for paclitaxel delivery. curcumin (CUR) derivative, methoxypolyethylene oxide-linked palmitate-modified curcumin (mPEO-CUR-PA), exhibited self-assemble into microspheres. The cytotoxic activity showed that paclitaxel encapsulated mPEO-CUR-PA microspheres possess up to 5 to 44-fold increase in vitro cytotoxicity (in terms of % cell mortality) in susceptible (HCC-S102 and A549) and paclitaxel-resistant (A549RT-eto) cancer cells, respectively, compared with that of free paclitaxel. Even the enhancement solubility and activity of curcumin and its derivative via many methods, encapsulation or general modified functional groups, have been demonstrated. However, the improvement of curcumin delivery in to cell is still studied.

2.8 Peptide nucleic acid (PNA)

Peptide nucleic acid (PNA) is an artificially synthesized polymer with the structure similar to those of deoxyribonucleic acid (DNA) or ribonucleic acid (RNA) except that the PNA backbone is N-(2-aminoethyl) glycine unit combined with peptide whereas the DNA backbone is ribose-phosphate backbone¹²⁹. The structure of PNA compared with that of DNA is illustrated in Figure 2.17. The PNA backbone is both chemically and biologically stable. Peptide bonds can make PNA readily conjugated with peptides, fluorescent dyes, and other useful molecules. Moreover PNA possess many properties that make them leading candidates, including a propensity for rapid and high-affinity binding^{130 131 132 133}, resistance to degradation by nucleases and proteases^{134 135 136}, poor affinity for proteins that normally bind nucleic acids, and high mismatch discrimination^{137 138}.

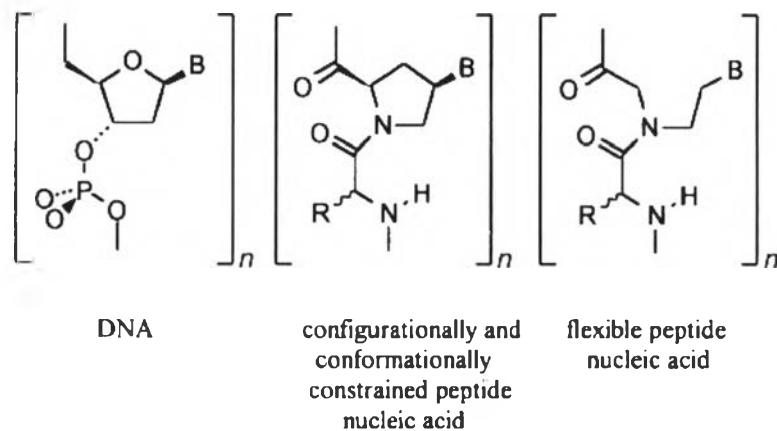


Figure 2. 15 Comparison of structure of the target peptide nucleic acids and DNA

The PNA/DNA or PNA/PNA duplex is more stable than the natural homo- or heteroduplexes because of the non-electrostatic backbone¹²⁹ followed by Watson-Crick complementary DNA, RNA (or PNA) oligomers^{130 131 132 133}. PNA can bind to complementary sequence of DNA and mRNA^{137 138}. It can break up DNA duplex and form PNA/DNA triplex or double duplexes without denaturing the DNA duplex¹³⁹ (Figure 2.18). PNA oligomers also show greater specificity in binding to complementary DNAs, with a PNA/DNA base mismatch being more destabilizing than

a similar mismatch in a DNA/DNA duplex¹³⁸. This binding strength and specificity also applies to PNA/RNA duplexes. PNAs are not easily recognized by either nucleases or proteases, making them resistant to enzyme degradation¹³⁴. PNAs are also stable over a wide pH range.

PNA Binding modes

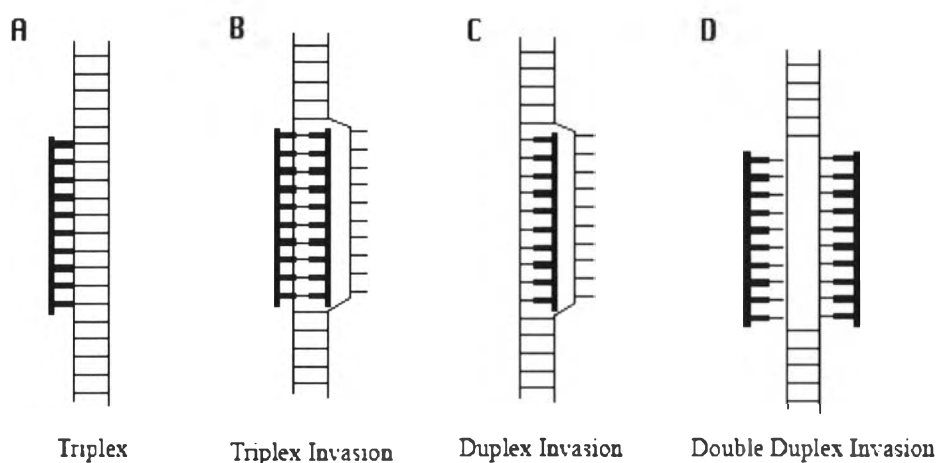


Figure 2. 16 PNA binding modes for targeting double stranded DNA Thick structures signify PNA¹³⁹

Owing to the PNA properties, both chemically and biologically stabilities, PNA were very attractive candidates for gene delivery system, especially in antisense technology¹⁴⁰. Subsequently, the design and synthesis of PNA have been to interest. In 1997 Lowe and Vilaivan¹⁴¹ reported the design and synthesis of amino acids bearing nucleobases, novel peptide nucleic acids. The synthesized PNA product, *N*-*tert*-butoxycarbonyl-*N*-(2-hydroxyethyl)glycine methyl ester, was achieved. The hydroxy group of this compound replaced with protected nucleobases using the Mitsunobu reaction. Moreover, In the same year, *N*-Fmoc-glycyl-4-(*N*⁶-benzoyladenine-9-yl)proline, *N*-Fmoc-glycyl-4-(*N*⁴-benzoylcytosine-1-yl)proline and *N*-Fmoc-glycyl-4-(*N*²-isobutylguanin-9-yl)proline and their pentafluorophenyl esters of the *cis*-D series were synthesized by Lowe and Vilaivan¹⁴². In 2001 Vilaivan and co-worker¹⁴³ developed a synthetic route for novel pyrrolidine PNAs bearing four different β -amino acid spacers. These PNAs comprising alternate sequences of nucleobase-modified D-

proline and β -amino acid spacers selected from L-aminopyrrolidine-2-carboxylic acid, D-aminopyrrolidine-2-carboxylic acid, (1*R*,2*S*)-2-aminocyclopentane carboxylic acid and β -alanine were synthesized using solid phase methodology. In 2002, Vilaivan and Lowe¹³⁸ reported a novel pyrrolidinyl PNA having a high affinity toward DNA and RNA in a sequence-specific fashion. Ten base pairs lysine-capped pyrrolidinyl PNA was synthesized and demonstrated that the PNA bound more specifically to the complementary DNA than RNA. This PNA/DNA or PNA/RNA duplex showed less toleration to the mismatch base pairing. Moreover, circular dichroism spectrum and UV titration showed that the PNA/DNA duplexes were in the form of B-type double helix Watson-Crick base pairing with 1:1 ratio. In 2005 Suparpprom and co-worker¹⁴⁴ synthesized rigid pyrrolidinyl peptide nucleic acids (PNA) based on D-prolyl-2-aminocyclopentanecarboxylic acid (ACPC) backbones. The binding properties of stereoisomeric PNAs possessing different stereochemistry at the ACPC part revealed that the stereochemistry of the backbone is very important. In addition, only the PNA containing (1*S*,2*S*)-ACPC can form a very stable 1:1 complex with the complementary DNA in a sequence-specific manner. In 2006 Vilaivan and co-worker¹³⁷ synthesized (1*S*,2*S*)-2-aminocyclopentanecarboxylic acid (acpcPNA) which bound strongly and selectively to complementary DNA in an exclusively antiparallel fashion. The acpcPNA preferred to bind to cDNA over cRNA. The PNA/DNA duplex strictly follows the Watson-Crick base-pairing rules.

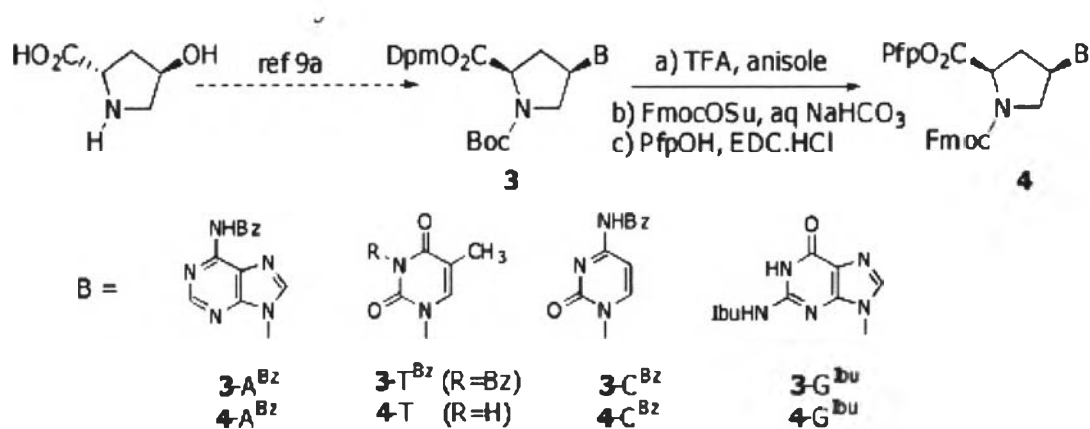


Figure 2. 17 Synthesis and structures of PNA monomers¹³⁷

In 2008 Siriwong and co-worker¹⁴⁵ using molecular dynamics simulations (MD) and melting temperature (T_m) analyses showed that pyrrolidinyl PNA bound strongly and selectively to complementary DNA in an antiparallel fashion. The pyrrolidinyl PNA binds to complementary DNA higher stable than DNA/DNA duplex.

Furthermore, the advantages that PNA offers new opportunities for drug delivery system in medical development field. Many research discussed the recent progress and future goals in developing therapeutic PNAs targeted against nucleic acid sequences. However, important issues regarding activity in vivo are still under investigation.

2.9 The development of PNA as anti-gene

Recently, PNAs can be delivered into cells by adapting a widely used technology. They are potentially useful for the regulation of gene expression which binds with DNA or mRNA. Consistent with the antisense and anti-gene principle¹⁴⁶, this explains a way to control protein synthesis at the nucleic acid level which should be much more effective than inhibition of enzymes. According to transcription, the gene in nucleus expresses a relatively large number of copies of messenger ribonucleic acid (mRNA). Then mRNA is translated into a large number of protein molecules. Therefore, the inhibition of gene expression must more efficient than inhibition of the resulting protein product. At present, many researches are designed a medicine which is based on direct interaction activity with DNA. The several medicines, such as adriamycin, bleomycin, or cisplatin, are unable to exhaust the sequence information contained in the nucleic acids and do not act specifically on particular genes. Consequently, the synthetic oligonucleotides can be used as a sequence-specific recognition of nucleic acids which is bind specifically by hydrogen bonding to complementary nucleic acids. These compounds are called anti-gene oligonucleotides based on their binding to the target sequence. Thus the therapeutic PNA must be properties followed by: (1) it must be sufficiently stable under physiological conditions, able to pass through the cell membrane, and bind specifically and tightly to the target nucleic acids¹⁴⁶. (2) it has been shown that PNAs



can block the access of restriction enzymes to their recognition sites¹⁴⁷. (3) it should also be possible to use PNAs to limit the access of DNA binding transcription factors.

Vickers and co-worker¹⁴⁸ showed triplex-forming PNAs to inhibit NF- κ B-specific transcriptional activation by duplex invasion. In 2000 Giovanna and co-worker¹⁴⁹ synthesized anti-*myc* PNA which is specific to *c-myc* oncogene. The anti-*myc* PNA was covalently linked with nuclear localization signal (NLS) (PNA-*myc*-NLS). The result showed 75% of inhibition of MYC expression at 10 mM PNA-*myc*-NLS concentration. In 2005 Tonelli and co-worker¹⁵⁰ developed an antigene peptide nucleic acid (PNA) for selective inhibition of *MYCN* transcription in neuroblastoma cells. The antigene PNA conjugated with a nuclear localization signal (NLS) peptide (PNA₅-NLS), designed specific to *MYCN* sequence. The result showed that *MYCN* expression was inhibited by PNA₅-NLS at 10 μ M. Moreover, for additional information on PNA chemistry, binding properties, applications in cancer therapy, and strategies to modulate gene expression^{151 152 153 154}. For anti-gene applications, the developing PNA is usually conjugated with cell penetrating peptides or lipophilic molecules to enhance cellular delivery because non-electrostatic backbone of PNA diffuses very slowly. In 2011 Gagnon and co-worker¹⁵⁵ synthesized oligonucleotide-oligospermine conjugates (Zip nucleic acids or ZNAs) for antisense and anti-gene agents. ZNAs was delivered by reverse transfection, cationic lipid, oligonucleotide and Lipofectamine RNAiMAX cationic lipid. The PR expression results showed ZNAs with lipid carriers suppressed PR expression at 50 nM. Moreover, ZNAs could be cell-permeable anti-gene agent at 500 nM. Macadangang and co-worker¹⁵⁶ synthesized PNA as anti-gene and prepared *in vitro*-packaged (IVP) PNA vectors by nucleocapsid protein derived from Simian virus 40. The result showed that delivered PNA suppressed *MDR1* gene expression at 10.7 μ M for 48 h. Therefore, specific sequence PNA is able to inhibit gene transcription by binding to a specific region on DNA which is a binding site of transcription factor.



2.10 Interleukin 6 (IL-6)

Interleukin 6 (IL-6) is a cytokine that plays important role in acute inflammatory response or injury and chronic inflammatory diseases. As shown in Figure 2.19, IL-6 can be induced in many cell types, including T cells^{157 158} and B cells^{159 160 161}, activated monocytes^{162 163}, endothelial cells^{164 165}, and cancer cells¹⁶⁶ in response to a variety of stimuli. Furthermore, it also plays a role in hematopoiesis, neuronal regeneration, fertility and immune response^{167 168}. In case of acute inflammation, IL6 is secreted into blood circulation. The expression of *il-6* gene is relate to inflammation which is induced by the bacterial endotoxin (lipopolysaccharide [LPS])^{163 166 169}, viral infection⁶⁹, or a variety of other cytokines like tumor necrosis factor a (TNF- α)^{138 170}, IL-1^{163 165 170 171}, and platelet-derived growth factor¹⁷¹.

To induce *il-6* gene expression, the promoter region of the *il-6* gene revealed the presence of a putative binding site for the NF- κ B transcription factor^{172 173}. As shown in Figure 2.18, the NF- κ B transcription factor was between -75 and -63¹⁷⁴. Then the action of NF- κ B on the IL-6 promoter mediates is relate to the regulation of IL-6 expression. Matsusaka and co-worker¹⁷⁵ studied on transcription factors NF-IL-6 and NF- κ B. They found that single binding sites for transcription factors NF-IL-6 and NF- κ B are present in the promoter of the *il-6* gene. Betts and co-worker¹⁷⁶ also reported that the interleukin-1 (IL-1) and interleukin-6 (IL-6) stimulated transcription from NF- κ B and NF-IL6 element binding factors individually.



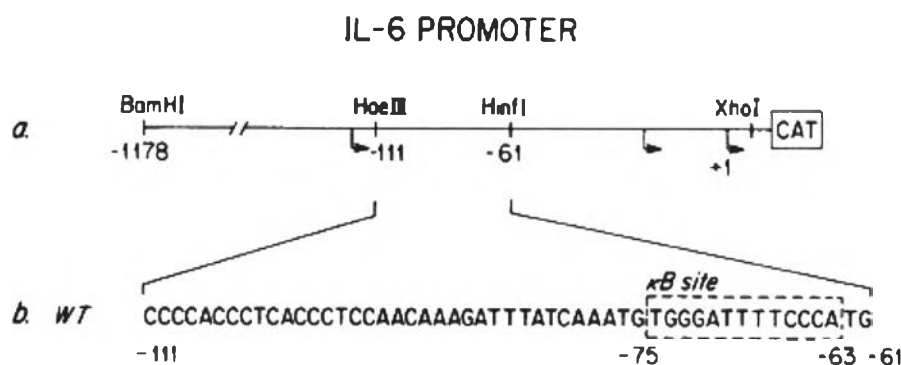


Figure 2. 18 Sequence of the IL-6 promoter. (a) Schematic diagram of the 5'-flanking region of the *il-6* gene. (b) Sequence of HaeIII-HinfI fragment of *il-6* gene (62). Box indicates sequence of NF- κ B-binding site¹⁷³

In relation to IL-6 expression, the previous studies have been reported many the technique for determining IL-6 expression, such as enzyme linked immunosorbent assay (ELISA), luciferase assay system, polymerase chain reaction (PCR) and quantitative real-time polymerase chain reaction (qRT-PCR). In 2005 Zamtetaki and co-worker¹⁷⁷ studied the IL-6 expression in human aorta smooth muscle cell by RNase protection assay (RPA) and ELISA. The result showed that IL-6 expression was related to Ras, Rac1, P38NAPK, NF-IL-6 and NF- κ B and was reversibly controlled by PKC- δ . The IL-6 expression was responsible for the tissue inflammation. Ropelle and co-worker¹⁷⁸ reported a mechanism dependent upon the pro-inflammatory cytokine interleukin 6 (IL-6) which is suppresses hyperphagia and associated hypothalamic IKKb/NF- κ B activation. The determination of IL-6 concentration used a commercially available ELISA kit. Tseng and co-worker¹⁷⁹ used oxidize 1-pamitoyl-2-arachidonyl-sn-glycero-3-phosphopoline (ox-PAPC) to control IL6 gene expression in murine calvarial preosteoblasts. The *il-6* gene expression was determined by qRT-PCR. The result showed that at 40 μ g/mL of the ox-PAPC could control *il-6* gene expression after 6 h incubation. A year later, Drygin and co-worker¹⁸⁰ used small interference RNA system designed specifically against CK2, upstream regulatory factor of IL-6 in human IBC cell line SUM-149PT. The aim of this report was to reduce IL-6 expression in human IBC cell line SUM-149PT as a model. The IL-6 expression was measured by qRT-PCR and OptEIA Human IL6 ELISA kit II.

As the promoter region of the *il-6* gene which is the presence of a putative binding site for the NF- κ B transcription factor. Targeting of this site was interested to design specifically inhibition of NF- κ B binding and suppressional transcription of IL-6. Grigoriev and co-worker¹⁸¹ demonstrated the inhibition of NF- κ B binding and transcriptional activation of the IL-2RaX promoter using an acridine-derivatized, methylcytosine substituted DNA oligonucleotide. After that, Vicker and co-worker¹⁴⁸ reported that PNA strand invasion offers an attractive alternative to DNA oligonucleotide directed triplex formation as a potential tool for gene inhibition. This PNA possesses capable of specifically blocking interaction of the transcription factor NF- κ B.

This work aimed to produce carbon-based nanomaterial with functionalize surface for biological applications. The production of the materials was to oxidized graphite using a novel method. The product was modified either by fluorescence dye labeling or absorption of actives. The products were thoroughly characterized for their morphology and chemical composition. Bio-applications as an *in vitro* drug nanocarrier of the newly obtained particles in drug delivery are demonstrated. The study is involved cytotoxicity evaluation of the carbon oxide nanocarriers, applications of the carbon oxide particles for the delivery of active ingredients including curcumin and peptide nucleic acid (PNA) into target cells and also the monitoring localization of both curcumin and nanocarriers once inside the cells.

Curcumin was selected for its good anticancer activity, auto-fluorescence, hydrophobicity, and poor solubility in water¹¹¹. The antitumor activity will be determined to confirm the delivery of curcumin into cancer cells. The other active ingredient used in this study is peptide nucleic acid (PNA) of type (1S, 2S)-2-aminocyclopentanecarboxylic acid (acpcPNA)¹³⁷. This acpcPNA can strongly and selectively binds to its complementary DNA (cDNA) better than other types of PNA¹³⁷¹³⁸. It should be noted here that up until now there is no report on the delivery of acpcPNA into cell's nucleus. In addition, the PNA was designed to complement with the interleukin 6 (IL-6) promoter¹⁷⁵ which, after binding, should reduce the expression of the *il-6* gene. Monitoring of reduced *il-6* expression can determine the activity of nuclease localized PNA.



2.11 Research objectives

The aims of this research can be summarized as follow:

1. To synthesize and characterize cluster of carbon nanospheres
2. To use the obtained carbon oxide nanospheres as carrier for curcumin and peptide nucleic acid (PNA) delivery
3. To track intracellular trafficking of curcumin-loaded and PNA-loaded carbon oxide nanospheres
4. To investigate bioactivity of curcumin-loaded and PNA-loaded carbon oxide nanospheres in mammalian cells

